Localization in Seemingly Sensory-Denied Environments through Spatio-Temporal Varying Fields

Jose Fuentes and Leonardo Bobadilla
Knight Foundation School of Computing and Information Sciences
Florida International University
Miami FL, USA
jfuen099@fiu.edu, bobadilla@cs.fiu.edu

Ryan N. Smith
Institute of Environment
Florida International University
Miami FL, USA
rysmith@fiu.edu

Abstract—Localization in underwater environments is a fundamental problem for autonomous vehicles with important applications such as underwater ecology monitoring, infrastructure maintenance, and conservation of marine species. However, several traditional sensing modalities used for localization in outdoor robotics (e.g., GPS, compasses, LIDAR, and Vision) are compromised in underwater scenarios. In addition, other problems such as aliasing, drifting, and dynamic changes in the environment also affect state estimation in aquatic environments. Motivated by these issues, we propose novel state estimation algorithms for underwater vehicles that can read noisy sensor observations in spatio-temporal varying fields in water (e.g., temperature, pH, chlorophyll-A, and dissolved oxygen) and have access to a model of the evolution of the fields as a set of partial differential equations. We frame the underwater robot localization in an optimization framework and formulate, study, and solve the state-estimation problem. First, we find the most likely position given a sequence of observations, and we prove upper and lower bounds for the estimation error given information about the error and the fields. Our methodology can find the actual location within a 95% confidence interval around the median in over 90% of the cases in different conditions and extensions.

Index Terms—Marine Robotics, Underwater Localization, Optimization, Partial Differential Equations, Spatio-temporal Fields.

I. Introduction

A central challenge in marine robotics missions is underwater localization. One significant barrier is that traditional sensor modalities used for state estimation in robotics are affected by lack of reception (for GPS and compasses), absence of visual landmarks (for vision), aliasing (for LIDAR), significant drifting (for IMUs), and dynamic changes in the environment. Common alternatives for underwater localization are acoustic sensors such as Doppler Velocity Logs (DVLs). However, in some scenarios, DVLs can not contact the ocean floor, and it can also be costly to equip a fleet due to their price range. Another and periodic constantly resurfacing to get a GPS reading.

This work is supported in part by the NSF grants IIS-2034123, IIS-2024733, and by the U.S. Dept. of Homeland Security 2017-ST-062000002.

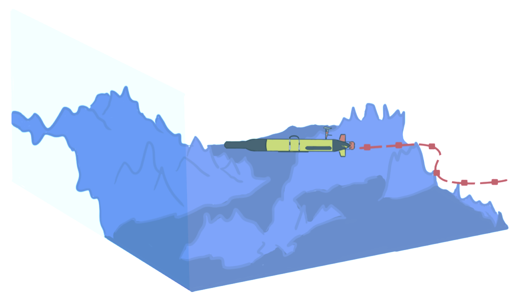

Fig. 1. Localization in an underwater environment.

However, this process is time and energy-consuming and can compromise stealth in covert missions. This paper proposes novel alternative state estimation algorithms for underwater robots equipped with sensors that can measure varying spatio-temporal fields in water (e.g., temperature, pH, chlorophyll-A, and dissolved oxygen). Besides these commonly used sensors, we also assume that the robot has a model of the evolution of the phenomena in the form of partial differential equations. We frame underwater robot localization in an optimization framework and formulate, study, and solve a state-estimation problem.

A. Related Work

Most underwater localization approaches rely on Bayesian filters such as Kalman Filters (and their extensions) and non-parametric particle filters. A review of these techniques can be found in [1]. Common modalities include acoustic localization or visual odometry [2] combined with dead reckoning. This paper aims to propose alternative state estimation approaches without an established infrastructure. Our ideas are also connected to state estimation approaches based on signal strength [3] and the construction of minimalist filters to solve robotics tasks [1].

Our research is connected to efforts to augment traditional Terrain-Based Navigation (TBN) methods developed before satellite-based navigation methods. To enhance the ability to navigate and localize, we have developed in our previous work an Augmented TBN (ATBN) that incorporates water parameter data (e.g., temperature, salinity, pH) to enhance the topographic scalar field that the vehicle uses to navigate under the traditional TBN framework [4]–[6]. The hypothesis is that including physical water data in the terrain map provides a more robust map. In this paper, we are extending our Augmented TBN models to be resilient to spatio-temporal dynamics.

To make the paper self-contained, we will introduce the mathematical notations and basics used in our methods in this section.

B. Partial differential equations (PDE)

Recently, the importance of mathematical modeling has reached crucial levels and PDEs have played a key role due to their adaptability and interpretability. They have been used to model different phenomena from socio-economic sciences [7], biology [8], and oceanography [9]–[11]. Phenomena such as pH, temperature, and salinity usually have been modeled using PDEs. Depending on their nature, diffusion, advection, or combination are used to model each phenomenon [12]–[14]. Consequently, it is important to examine how those phenomena behave given certain initial conditions. Here, each phenomenon is a scalar field $f : \mathbb{R}^2 \times [0, \infty) \longrightarrow \mathbb{R}$. One of the most used models for the evolution of these scalar fields is the advection equation given by

$$\begin{aligned} \frac{\partial f}{\partial t} + b \cdot \nabla f &= g(x,t), \text{ for } (x,t) \in \mathbb{R}^2 \times (0,\infty) \\ f(x,0) &= h(x), \text{ for } t = 0 \end{aligned} \tag{1}$$

which has the solution

$$f(x,t) = h(x - tb) + \int_0^t g(x + (s-t)b, s)ds \tag{2}$$

provided that $g(x,t) \in C(\mathbb{R}^2)$ and it has a compact support.

Another important model is the diffusion equation, inspired by the heat diffusion problem, for $\mathbb{R}^2$. It is given by

$$\begin{aligned} \frac{\partial f}{\partial t} - \Delta f &= g(x,t), \text{ for } (x,t) \in \mathbb{R}^2 \times (0,\infty) \\ f(x,0) &= h(x), \text{ for } t = 0. \end{aligned} \tag{3}$$

It has the solution

$$\begin{aligned} f(x,t) = & \int_{\mathbb{R}^2} \Phi(x-y,t)h(y)dy \\ & + \int_0^t \int_{\mathbb{R}^2} \Phi(x-y,t-s)h(y,s)dyds \end{aligned} \tag{4}$$

where $\Phi(x,t)$ is called the fundamental solution for the heat equation and it is given by

$$\Phi(x,t) = \begin{cases} \frac{1}{4\pi t}\exp(-\|x\|^2/4t) & \text{if } x = 0 \\ 0 & \text{if } x = 0 \end{cases} \tag{5}$$

II. Problem Formulation

Our problem is motivated by a scenario in which a robot moves in an underwater 2-dimensional plane and needs to localize. In our formulation, we have one robot, which is moving in a two-dimensional open and bounded space $D \subset \mathbb{R}^2$. The robot does not have access to traditional sensors used for localization (e.g., GPS), but it has sensors capable of measuring different water parameters, such as pH, temperature, and salinity at a given time $\hat{t}$. Each of those is a known scalar function $f_k(x,t) : D \rightarrow \mathbb{R}$, which is a solution of (1). This feature provides physical and realistic modeling of a spatio-temporal field. Also, $1 \leq k \leq m$ and m are the numbers of those characteristics which the robot can measure. Therefore, the robot at each time $\hat{t}$ returns a set of observations $y^{\hat{t}} = (y_1^{\hat{t}}, \ldots, y_m^{\hat{t}})^\top \in \mathbb{R}^m$ at the point where it is located. This motivates our problem of interest.

Robot localization in spatio-temporal fields problem

Given a set of (likely noisy) observations $y^{\hat{t}}$ and a set of functions $\{f_1(x,\hat{t}), \ldots, f_m(x,\hat{t})\}$ modeling each phenomenon find the current location of the robot in the domain D.

III. Methods

To address the problem of localizing in spatio-temporal fields we define the function $F(x,\hat{t}) = (f_1(x,\hat{t}), \ldots, f_m(x,\hat{t}))^\top$ for a fixed time $\hat{t}$. Hence, the problem can be posed as:

$$\begin{aligned} F(x,\hat{t}) &= y^{\hat{t}} \\ \text{s.t.} \quad & x \in D. \end{aligned} \tag{6}$$

Nevertheless, solving this equation using some method (e.g., Newton) has several problems. First, if we consider Newton's method, it uses the inverse of the Jacobian function to compute the solution x. Usually, it is necessary to restrict the number of functions to the number the variables (2 in this case). Second, since solving this non-linear equation requires an iterative method, the method tends to diverge if the starting point is far from one solution. Third, it is not possible to handle corrupted observations using this approach. Therefore, if the Jacobian has a high condition number, it leads to inaccurate system solutions.

Therefore, to handle these problems, we propose an optimization formulation. First, using a metric d defined on $\mathbb{R}^m$, the aim is to solve the minimization problem

$$\begin{aligned} \min_{x \in \mathbb{R}^2} \quad & d(F(x,\hat{t}), y^{\hat{t}}) \\ \text{s.t.} \quad & x \in D. \end{aligned} \tag{7}$$

This approximation provides a manner to soften the direct approach given in (6). Those methods, namely regularization methods have become popular in handling ill-posed problems and converting them into optimization problems. Here, the metric determines the priorities in the optimization problem. it determines the nature and some properties of the optimization problem solution. The most used metric is the L^2 norm because of its derivative properties. It is possible to use a different biased metric toward one measure. This optimization problem includes (6) problem, if there is any $x \in D$ solving (6), therefore, x solves the problem (7). Also, the problem allows having approximated locations to the given observations.

Also, we are interested in studying the scope of this approach through bounding the error if we consider noisy observations. The following section aims to give bounds and approximations of the optimal solutions, considering sensor noise in the measurements (i.e. corrupted data or sensor deficiencies). For this reason, we will define the notation used henceforth.

- We will refer to the functions $f(x, \hat{t})$ and $F(x, \hat{t})$ as $f(x)$ and $F(x)$ keeping in mind that those phenomena are considered in the fixed time $\hat{t}$ and that therefore they are modeling spatio-temporal phenomena. In addition, the gradient and the Hessian matrix, given a scalar function $f(x)$ will be named $\nabla f(x)$ and $H_f(x)$ respectively. In the case of a vectorial function $F(x, \hat{t})$, we name the Jacobian matrix as $J_F(x)$. Lastly, we rename $y^{\hat{t}}_i$ and $y^{\hat{t}}$ as y_i and y.
- In this case, $d(x, y) = \|x - y\|$ with $x, y \in R^n$ is the L^2 norm. Furthermore, if A is a matrix then, $\|A\|$ is the matrix subordinate norm defined as

$$\|A\| = \sup_{\|x\|=1} \|Ax\| = \sigma_{max}(A). \tag{8}$$

Where $\sigma_{max}(A)$ is the largest singular value of A.

A. Main results

Now, we present the main results (and contributions) of this work. The first two results are considered negative results. However, the third result is a way to “fix” those negative results into an upper and a lower bound. We consider a model of the sensors where each observation can be perturbed by cap-ture noise or sensor limitations or deficiencies. Therefore, each collection of measurements y is modeled as $y = F(x^*) + E$ where $F(x^*)$ is the real measurement at the real location and $E \sim N(0, \Sigma)$ is the multivariate normal distribution and Σ a diagonal covariance matrix to take into account the perturbations over the measurements described before.

Proposition 1. Let x^* the real location, $y = F(x^*) + E$ the corrupted set of observations, where $y = (y_1, \ldots, y_m)^*$, $F = (f_1(x^*), \ldots, f_m(x^*))^*$, $E = (\varepsilon_1, \ldots, \varepsilon_m)^*$ and $y_i = f_i(x^*) + \varepsilon_i$ the corrupted observation of the phenomenon i. Also, let x^*_E the solution of (7) with and D a convex and compact set. Then,

$$\max_{i=1,\ldots,m} \left(\frac{|\varepsilon_i|}{\max_{x \in D} \|\nabla f_i(x)\|} \right) \leq \|x^*_E - x^*\|. \tag{9}$$

Proof. We consider the best case of (7), that is, when the difference is precisely $y - F(x^*) = E$. Therefore, the functional achieves the value $||E||$. In consequence, we have that

$$f_i(x^*_E) = f_i(x^*) + \varepsilon_i. \tag{10}$$

By the mean value theorem there is a $\zeta_i \in (0, 1)$ such that

$$f_i(x^*_E) - f_i(x^*) = \nabla f_i((1 - \zeta_i)x^*_E + \zeta_i x^*) \cdot (x^*_E - x^*) \tag{11}$$

and the Cauchy-Schwartz inequality

$$\begin{aligned} |f_i(x^*_E) - f_i(x^*)| &\leq \|\nabla f_i((1 - \zeta_i)x^*_E + \zeta_i x^*)\| \|x^*_E - x^*\| \\ &\leq \max_{x \in D} \|\nabla f_i(x)\| \|x^*_E - x^*\|. \end{aligned} \tag{12}$$

Then,

$$\frac{|\varepsilon_i|}{\max_{x \in D} \|\nabla f_i(x)\|} \leq \|x^*_E - x^*\|. \tag{13}$$

Since this occurs for each i, we have that

$$\max_{i=1,\ldots,m} \left(\frac{|\varepsilon_i|}{\max_{x \in D} \|\nabla f_i(x)\|} \right) \leq \|x^*_E - x^*\| \tag{14}$$

as desired. □

This deterministic result allows us to estimate the error between the noisy solution and the actual location if we know a bound for the noise in each phenomenon. On the other hand, if we consider the random nature of each ε_i, we are interested in bounding $E[\|x^*_E - x^*\|]$, and therefore we can state the following derived result for random variables.

Proposition 2. Let x^*, x^*_E, E, $F(x)$ and D as in the Proposition 1 with $E \sim N(\mu, \Sigma)$, $\varepsilon_i \sim N(\mu_i, \sigma^2_i)$ and $m_i = \max_{x \in D} \|\nabla f_i(x)\|$, then,

$$\max_{i=1,\ldots,m} \left(\sqrt{\frac{2\sigma_i^2}{\pi m_i^2}} \exp\left(\frac{-\mu_i^2}{2\sigma_i^2}\right) + \mu_i \operatorname{erf}\left(\frac{\mu_i}{\sqrt{2\sigma_i^2}}\right) \right) \leq E[\|x^*_E - x^*\|] \tag{15}$$

where $\operatorname{erf}(x)$ is the error function defined by

$$\operatorname{erf}(x) = \frac{2}{\sqrt{\pi}} \int_0^x e^{-t^2} dt. \tag{16}$$

Proof. Starting from the inequality (13) we use the property of the integrals preserving inequalities. That is, if $f(x) \leq g(x)$, then, $\int_{R^n} f(x)dx \leq \int_{R^n} g(x)dx$. We obtain

$$\begin{aligned} &\int_{R^m} \frac{|\varepsilon_i|}{\max_{x \in D} \|\nabla f_i(x)\|} p(\varepsilon_1, \ldots, \varepsilon_m) d\varepsilon_1 \cdots d\varepsilon_m \leq \\ &\int_{R^m} \|x^*_E - x^*\| p(\varepsilon_1, \ldots, \varepsilon_m) d\varepsilon_1 \cdots d\varepsilon_m = E[\|x^*_E - x^*\|] \end{aligned} \tag{17}$$

for each i. By virtue of Fubini’s Theorem (here, we are assuming that the expected value exists i.e. the integral (17) converges) we can reorder (17) as the nested “double” integral

$$\int_{\mathbb{R}^m} \frac{|\varepsilon_i|}{\max_{x\in D}\|\nabla f_i(x)\|} p(\varepsilon_1,\dots,\varepsilon_m)\,d\varepsilon_1\cdots d\varepsilon_m = \frac{1}{\max_{x\in D}\|\nabla f_i(x)\|}\int_{\mathbb{R}}|\varepsilon_i|\left[\int_{\mathbb{R}^{m-1}} p(\varepsilon_1,\dots,\varepsilon_m)\,d\hat{\varepsilon}_i\right]d\varepsilon_i \tag{18}$$

where $d\hat{\varepsilon}_i = d\varepsilon_1\cdots d\varepsilon_{i-1}d\varepsilon_{i+1}\cdots d\varepsilon_m$. The inner term of (18) is the marginal probability of ε_i i.e. its probability density function $p(\varepsilon_i)$. So, we have that the right hand term of (18) is $E[|\varepsilon_i|]$ multiplied by a factor. Joining (17) and (18) we have the inequality

$$\frac{1}{\max_{x\in D}\|\nabla f_i(x)\|}E[|\varepsilon_i|] \le E[\|x_E^* - x^*\|]. \tag{19}$$

The random variable $|\varepsilon_i|$ follows a folded normal distribution $|\varepsilon_i| \sim FN(\mu_i, \sigma_i^2)$ [15]. Writing its expectation value explicitly we obtain the bound

$$\sqrt{\frac{2\sigma_i^2}{\pi M_i^2}}\exp\left(\frac{-\mu_i^2}{2\sigma_i^2}\right) + \mu_i \operatorname{erf}\left(\frac{\mu_i}{\sqrt{2\sigma_i^2}}\right) \le E[\|x_E^* - x^*\|] \tag{20}$$

$i = 1,\dots,m$. Using the argument as before to obtain (14) from (13) we have the desired result. □

Proposition 2 gives a probabilistic approach to our problem, but it seems to be ignoring the covariances between random variables. However, it is not since the results are in terms of the maximum and the maximum values of the semi-positive matrix Σ are found on its diagonal. Actually, using the Cauchy-Schwartz inequality the variances outweigh the covariances $\mathrm{Cov}[\varepsilon_i,\varepsilon_j] = \Sigma_{ij} \le \sqrt{\Sigma_{ii}\Sigma_{jj}} = \sigma_i\sigma_j$. Similarly, regarding to F and f_i we can change the term $\max_{x\in D}\|\nabla f_i(x)\|$ by the term $\max_{x\in D}||J_F(x)||$, nevertheless the first term gives us a more narrow bound for the error, so it is better for our purposes.

Now, we can assume that the random variables have zero mean if we know them beforehand because we can correct the measurements by the mean of random variable ε_i, which models the measurement i. Therefore, the study case when the random variables have zero mean is a corollary from Proposition 2.

Corollary 1. Let x^*, x_E^* and D, E, $F(x)$ as in the Proposition 1 with $E \sim N(0,\Sigma)$, $\varepsilon_i \sim N(0,\sigma_i^2)$ and $m_i = \max_{x\in D}\|\nabla f_i(x)\|$, then,

$$\max_{i=1,\dots,m}\left\{\sqrt{\frac{2\sigma_i^2}{\pi m_i^2}}\right\} \le E[\|x_E^* - x^*\|]. \tag{21}$$

We have proven two negative results since both are lower error bounds. However, we would like to have an upper bound of the error. This can be very difficult if we have large level sets for the functions f_i. Therefore, to simplify the analysis, we show an approximate upper bound of the error.

Proposition 3. Let x^*, x_E^*, ε_i, $f_i(x) \in C^2(D)$ and D as in the Proposition 1, then,

$$\|x_E^* - x^*\| \approx C(E) \le K\|E\|. \tag{22}$$

Where K depends on $F(x^*)$, $J_F(x^*)$ and x^*.

Proof. We notice that x is a solution of (7) if and only if x is a solution of the following problem

$$\min_{x\in D}\ \frac{1}{2}\|F(x) - y\|^2. \tag{23}$$

The problem (23) is easier to work than (7), since we are avoiding the square root derivative in the origin. Therefore, any solution x_E^* of (23) satisfies the first order conditions

$$J_F^T(x_E^*)(F(x_E^*)\underbrace{-F(x^*) - E}_{-y}) = 0. \tag{24}$$

Let $G,H : D \longrightarrow \mathbb{R}^2$ defined as $G(x) = J_F(x)^T(F(x) - F(x^*))$ and $H(x) = J_F(x)^T E$, so, (24) can be written as

$$G(x_E^*) - H(x_E^*) = 0 \tag{25}$$

with $G(x^*) = 0$. Keeping this in mind, we expand $G(x) - H(x)$ in its Taylor series

$$\begin{aligned} G(x_E^*) - H(x_E^*) = {} & G(x^*) - H(x^*) \\ & + (J_G(x^*) - J_H(x^*))(x_E^* - x^*) \\ & + o(\|x_E^* - x^*\|^2). \end{aligned} \tag{26}$$

Using (25) and discarding the residual term we have that

$$x_E^* - x^* \approx (J_G(x^*) - J_H(x^*))^{-1}H(x^*) = C(E). \tag{27}$$

We bound $K(E)$ using the consistency property of the induced matrix norm (see [16])

$$\begin{aligned} \|C(E)\| &= \|(J_G(x^*) - J_H(x^*))^{-1}H(x^*)\| \\ &\le \|(J_G(x^*) - J_H(x^*))^{-1}\|\,\|H(x^*)\| \\ &= \|(J_G(x^*) - J_H(x^*))^{-1}\|\,\|J_F(x^*)E\| \\ &\le \|(J_G(x^*) - J_H(x^*))^{-1}\|\,\|J_F(x^*)\|\,\|E\|. \end{aligned} \tag{28}$$

Then, we have one upper bound for $C(E)$. Also, it is possible to discard the term $J_H(x^*)$ if $\|E\|$ is small enough compared to $\|J_H(x^*)\|$ and $\|J_G(x^*)\|$ leading to the bound approximation

$$\|K(E)\| \le \|J_G(x^*)^{-1}\|\,\|J_F(x^*)\|\,\|E\|. \tag{29}$$

We notice that if a matrix A has inverse, the eigenvalues of the matrix $A^{-1}A^{-1^T} = (A^TA)^{-1} = (AA^T)^{-1}$ are the multiplicative inverse of the eigenvalues of the matrix AA^T. Hence, the maximum singular value of A^{-1} is the inverse of the lowest eigenvalue of A, leading to the bound

$$\begin{aligned} \|C(E)\| &\le \|J_G(x^*)^{-1}\|\,\|J_F(x^*)\|\,\|E\| \\ &= \underbrace{\frac{\sigma_{max}(J_F(x^*))}{\sigma_{min}(J_G(x^*))}}_{K}\|E\| \end{aligned} \tag{30}$$

as desired. □

In practice, propositions 1, 2, and 3 can be used to estimate error bounds once our method is applied. It allows some control and knowledge about the magnitude of the possible discrepancies due to the corrupted or noisy observations with the actual locations.

IV. Experimental results

We present several computational experiments of the proposed method using different noise levels. The simulation scheme is composed of a selection of a random time $\hat{t} \in [0, 100]$ and the domain $D = [0, 200] \times [0, 200]$. Then, a random real location $x^\star \in D$ is selected. Here, we modeled three phenomena $f_i(x, \hat{t})$ using functions that satisfy the advection equation 1.

A. Noise

To assess the proposed model, we computed the real observations $F(x^\star, \hat{t})$. Next, there are computed corrupted observations $y^{\hat{t}} = F(x^\star, \hat{t}) + E$. Lastly, we solve the optimization problem (7). We used a fixed time $\hat{t}$ and 1000 random locations to test the performance of the presented method.

B. Support of the functions

A hypothesis in this work is that the measurements should be close to the support of the function, we should have measurements far from zero in absolute value, and we addressed this part in the results section. This makes sense since the super-level sets $L_c^+(f)$ defined as $L_c^+(f) = \{x \in \mathbb{R}^2 : f(x) \geq c\}$ tend to be smaller for higher values for exponential functions, in addition, the sub-level sets $L_c^-(f)$ defined as $L_c^-(f) = \{x \in \mathbb{R}^2 : f(x) \leq c\}$ are big when they contain values close to zero.

Therefore, we performed tests constraining different portions of the support. Namely, we are considering those measures that are bigger than $\delta \in \{20, 50\}$ in absolute value. Essentially, we are considering values lying within the intersection

$$\bigcap_{i=1}^{3} L_\delta^+(f_i) \cup L_{-\delta}^-(f_i) \quad . \tag{31}$$

C. Direction and magnitude of the advection

Lastly, the models we are considering are solutions to the advection equation (1), which have the shapes derived from the fundamental diffusion equation solution (3). Keeping in mind that the transport direction is a key part of the advection equation, we tested two types of motion, changing the directions in which the functions are moving to. First, three vectors separated by $\frac{\pi}{4}$ radians starting by the vector $[1, 0]$ in the counterclockwise direction i.e.: $[1, 0]$, $[1, 1]$ and $[0, 1]$. Second, vectors pointing the same direction $[1, 1]$ but with different magnitudes.

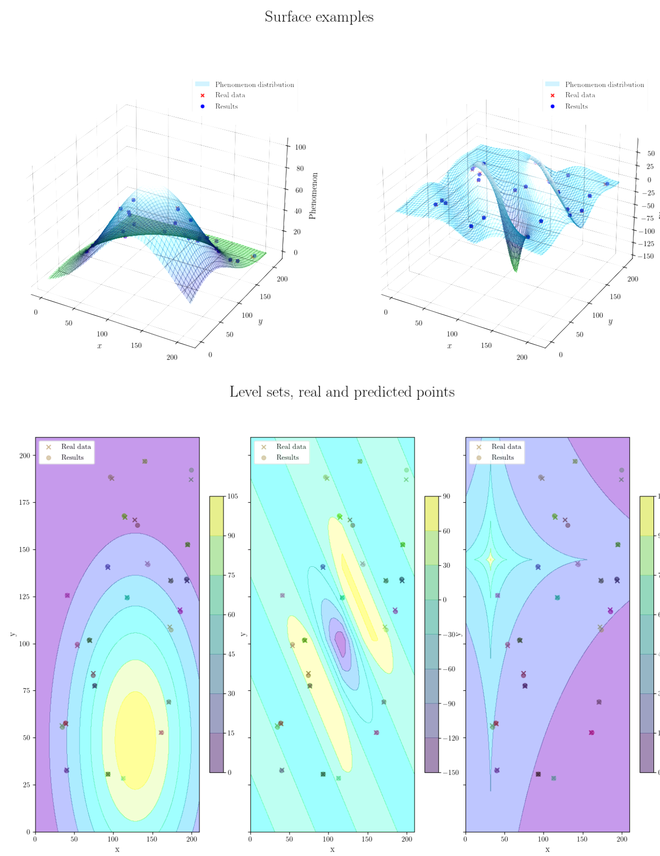

Fig. 2. Qualitative results. Top shows examples of surfaces representing the phenomena, solutions to Eq. (1) in a fixed time $\hat{t}$. The bottom presents the level sets of the surfaces with the predicted and real points.

D. Qualitative and quantitative results

Fig 2 presents qualitative results from our simulation. The proposed method is tested using functions that solve (1) and have similar shapes to the fundamental solutions for the heat equation (3).

Although these are qualitative results, we can observe that the most accurate predictions are made when the observations are close to the support of the three functions (see Fig. 2). This is important because points far from the support can be confused with points in the surroundings, which have similar values for the observations. Also, we observe that using this methodology it is possible to combine different sources of information to estimate the current location. Even, if necessary it is possible to change the functional $\hat{F}(x, t)$ defined in (7) to weight the uncertainty or precision of each phenomenon.

The results show in Fig 3 that localization performance is better closer to the support of the function. Also, it reflects that as long as the level sets (and therefore the support) the problem may become less accurate. Furthermore, it is possible to appreciate that the direction of the advection process considerably affects the performance. A possible explanation for this is that the distance between supports becomes bigger as time passes, reducing the search area.

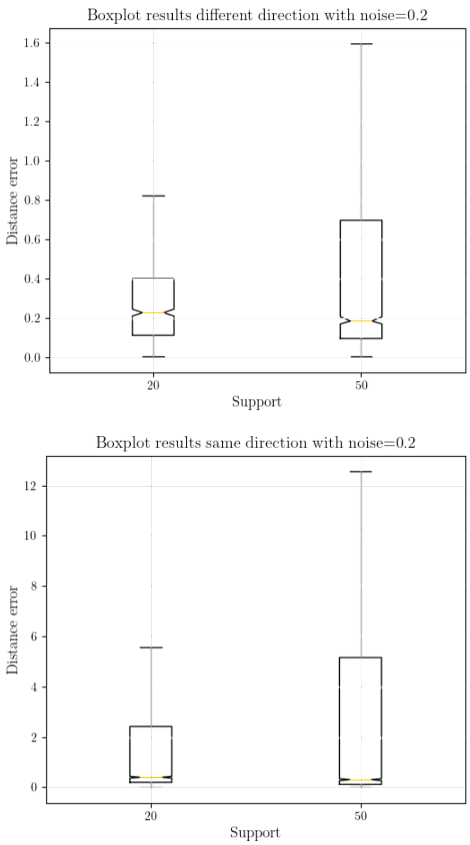

Fig. 3. Quantitative results of Problem 1 using different directions (top) and same direction (bottom), noises, and supports for the functions. The orange line corresponds to the median, the whisker to the interquartile range, and the notches determine the interval of 95% confidence around the median.

V. Conclusions and Future Work

In this paper, we presented a new method to localize a robot in an environment where it is impossible to get accurate GPS signals or bathymetry measures using environment-modeled spatio-temporal data collected by the robot. We studied the implications of the presented method theoretically, giving bounds of the estimation errors given noisy observations.

PDEs posed considering different domains can be quite difficult to deal with. Unfortunately, to solve each problem, it is necessary to define a function that depends on the domain and the equation itself. This function is called Green's function, and it takes advantage of Duhamel's principle [12], [13] to give a closed solution form. Nevertheless, this function has more theoretical purposes than practical ones. In this sense, it is reasonable to think that the solutions in different domains may have similar forms to the fundamental solutions.

In the near term, we will consider different PDE models to consider richer and more dynamic environments. Also, PDEs perform well when the initial condition $h(x)$ and the parameters governing its behavior b, $g(x,t)$ are known. However, those parameters should be calculated or estimated beforehand and updated if possible. We would like to explore the usage of satellite data, more models, and regularization techniques to estimate these parameters.

Acknowledgment

The authors want to thank the members of the MORA lab for giving constructive comments for this work.

References

[1] S. M. LaValle et al., "Sensing and filtering: A fresh perspective based on preimages and information spaces," Foundations and Trends® in Robotics, vol. 1, no. 4, pp. 253–372, 2012.

[2] P. Corke, C. Detweiler, M. Dunbabin, M. Hamilton, D. Rus, and I. Vasilescu, "Experiments with underwater robot localization and tracking," in Proceedings 2007 IEEE International Conference on Robotics and Automation. IEEE, 2007, pp. 4556–4561.

[3] B. Ferris, D. Fox, and N. D. Lawrence, "Wifi-slam using gaussian process latent variable models." in IJCAI, vol. 7, no. 1, 2007, pp. 2480–2485.

[4] A. J. Bayuelo, T. Alam, G. M. Reis, L. F. Niño, L. Bobadilla, and R. N. Smith, "Toward simultaneous localization and mapping in aquatic dynamic environments," in OCEANS 2019-Marseille. IEEE, 2019, pp. 1–5.

[5] M. Fitzpatrick, G. M. Reis, J. Anderson, L. Bobadilla, W. Al Sabban, and R. N. Smith, "Development of environmental niche models for use in underwater vehicle navigation," IET Cyber-systems and Robotics, vol. 2, no. 2, pp. 67–77, 2020.

[6] G. M. Reis, M. Fitzpatrick, J. Anderson, L. Bobadilla, and R. N. Smith, "Augmented terrain-based navigation to enable persistent autonomy for underwater vehicles," in Robotic Computing (IRC), IEEE International Conference on. IEEE, 2017, pp. 292–298.

[7] M. Burger, L. Caffarelli, and P. A. Markowich, "Partial differential equation models in the socio-economic sciences," p. 20130406, 2014.

[8] N. I. Kavallaris and T. Suzuki, "Non-local partial differential equations for engineering and biology," Mathematical modeling and analysis (Mathematics for Industry, vol. 31, 2018.

[9] L. Tartar, "Partial differential equations models in oceanography," 1999.

[10] N. Rakowsky, "The schur complement method as a fast parallel solver for elliptic partial differential equations in oceanography," Numerical linear algebra with applications, vol. 6, no. 6, pp. 497–510, 1999.

[11] T. K. Akinfe and A. C. Loyinmi, "An improved differential transform scheme implementation on the generalized allen-cahn equation governing oil pollution dynamics in oceanography," Partial Differential Equations in Applied Mathematics, vol. 6, p. 100416, 2022.

[12] L. Bers, F. John, and M. Schechter, Partial differential equations. American Mathematical Soc., 1964.

[13] L. C. Evans, "Partial differential equations," Graduate studies in mathematics, vol. 19, no. 4, p. 7, 1998.

[14] J. L. Martin and S. C. McCutcheon, Hydrodynamics and Transport for Water Quality Modeling, 1st ed., S. Wood, Ed. CRC Press, Inc., 1999.

[15] M. Tsagris, C. Beneki, and H. Hassani, "On the folded normal distribution," Mathematics, vol. 2, pp. 12–28, 3 2014.

[16] D. Kincaid, D. R. Kincaid, and E. W. Cheney, Numerical analysis: mathematics of scientific computing. American Mathematical Soc., 2009, vol. 2.

[17] H.-P. Tan, R. Diamant, W. K. Seah, and M. Waldmeyer, "A survey of techniques and challenges in underwater localization," Ocean Engineering, vol. 38, no. 14-15, pp. 1663–1676, 2011.

[18] G. M. Reis, M. Fitzpatrick, J. Anderson, L. Bobadilla, and R. N. Smith, "Increasing persistent navigation capabilities for underwater vehicles with augmented terrain-based navigation," in MTS/IEEE Oceans, 2017.

[19] Y. Mileyko, G. Reis, M. Chyba, and R. N. Smith, "Energy-efficient control strategies for updating an augmented terrain-based navigation map for autonomous underwater navigation," in Control Technology and Applications (CCTA), 2017 IEEE Conference on. IEEE, 2017, pp. 223–228.

[20] S. C. Endres, C. Sandrock, and W. W. Focke, "A simplicial homology algorithm for lipschitz optimisation," Journal of Global Optimization, vol. 72, pp. 181–217, 10 2018.

[21] A. Alvi, B. Ru, J.-P. Calliess, S. Roberts, and M. A. Osborne, "Asynchronous batch bayesian optimisation with improved local penalisation," in International Conference on Machine Learning. PMLR, 2019, pp. 253–262.

[22] E. L. Lima, Análise no Espaço Rn, 2nd ed. IMPA, 2016.

[23] S. M. LaValle, Planning algorithms. Cambridge university press, 2006.